



7

Conus Mediterraneus conch anisotropic structure and its effect on nanomechanical properties

Cristina Bignardi¹, Michele Petraroli and Nicola M. Pugno^{2,3}

¹Mechanical Department, Politecnico di Torino, Corso Duca degli Abruzzi 24
10129, Torino, Italy; ²Department of Structural Engineering and Geotechnics
Politecnico di Torino, Corso Duca degli Abruzzi 24, 10129, Torino, Italy

³National Institute of Nuclear Physics – National Laboratories of Frascati
Via E. Fermi 40, 00044, Frascati, Italy

Abstract

Nanoindentation has been used to explore, at the nanoscale, the mechanical properties of the Conus Mediterraneus conch, in order to compare nanohardness and elastic modulus with respect to its microstructural anisotropic architecture. For the experimental tests a Nano Indenter XP (MTS Nano Instruments, Oak Ridge TN) has been used. The mechanical tests have been

carried out on the inner and outer surfaces of the shell, as well as on its cross section, near to the inner/outer surfaces and in the middle layer. The results confirm the three layered anisotropic architecture of the investigated conch. On each of these 5 surfaces, 2x5 indentations have been performed at different maximum depth: from 250 nm to 4 μm , with a step of 250 nm, for a total of 800 tests. The numerous observations have been analysed applying an ad hoc modification of the Weibull Statistics, suggesting a natural evolution of the conch against external attacks.

1. Introduction

Growth and self-strengthening of natural materials is very attractive. According to Darwin, the reason for the survival of living organisms is that they could evolve and improve themselves in such a way to be always compatible with the environment. Therefore, in such a sense, it is no doubt that natural materials are the most optimized materials in the world. Their structures are highly integrated in natural organisms, such as biological hard tissues (bone, tooth, mollusc shell, bark, etc.) [1]. The laminated organization of these structures is inherent at different spatial scales (nano, micro, meso, macro). They all exhibit special properties and functions. From the view-point of the material scientist, it is beneficial to learn from these natural materials and structures. Learning from Nature has become now one of the most fascinating subjects in material research.

2. Conch shell structure

Sea shells are composed of calcium carbonate crystals interleaved with layers of viscoelastic proteins, having dense, tailored structures that yield excellent mechanical properties [2, 3]. Shells have architectures that differ depending on growth requirements and shell formation of the particular mollusc.

Conus Mediterraneus conch shells, Figure 1, have a cross-lamellar structure that consists of lath-like aragonite crystals (99.9 wt%) and a tenuous organic layer (0.1 wt%) [4]. The microstructures of conch shell are organized in three macro-layers (Figure 2) [1]. Each macro-layer consists of many crossed first-order lamellae, each of them composed by second-order lamellae. Furthermore, the second-order lamella is made up of third-order lamellae, which are single- or multi-crystals. Further analysis indicates that each lamella is connected to its neighbor lamellae by a proteinaceous adhesive. The first-order lamellae have thickness of 5–30 μm and are several micrometers wide, while the second-order ones are about 5 μm thick and 5–30 μm wide; the third order lamellae are nanosized. Thus, the thickness of the lamellae varies to some extents. In some



Figure 1. Conus Mediterraneus conch.

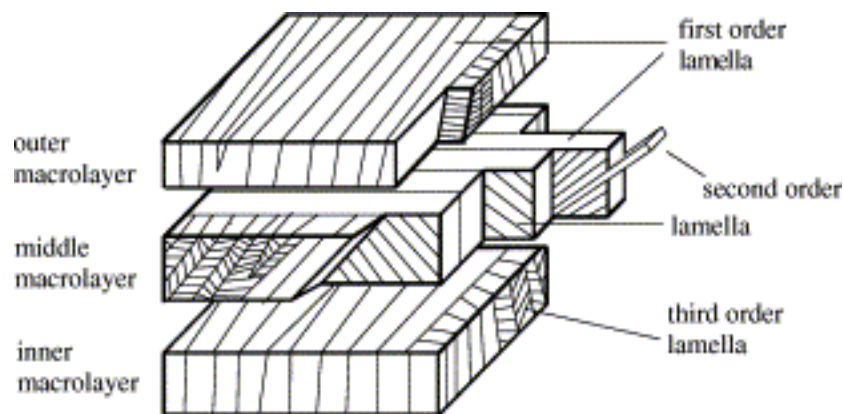


Figure 2. Schematic diagram of crossed-lamellar three layered anisotropic architecture of conch shell.

zones lamellae become rather thinner or eventually disappear. Each lamella consists of lath-like crystals. The hierarchical lamellae have different orientations. Moreover, the lamellae are rotated in the “lamellar plane” of an angle of about 70–90° with respect to their neighbor layer(s). The complete microscopic composite sketch map of conch shell is shown in Fig. 2.

3. Materials and methods

Nanoindentation method has been used to explore, at the nanoscale, the mechanical properties of the Conus Mediterraneus conch (Fig. 1) in order to compare nanohardness and elastic modulus with respect to its microstructural anisotropic architecture (Fig. 2).

For the experimental tests a Nano Indenter XP (MTS Nano Instruments, Oak Ridge TN, Figure 3) has been used. The mechanical tests have been carried out on the inner/outer surfaces of the shell and on three zones along its cross section (inner, middle and outer) in order to determine the nanohardness and Young’s modulus by varying position and orientation, Figure 4. Specimens

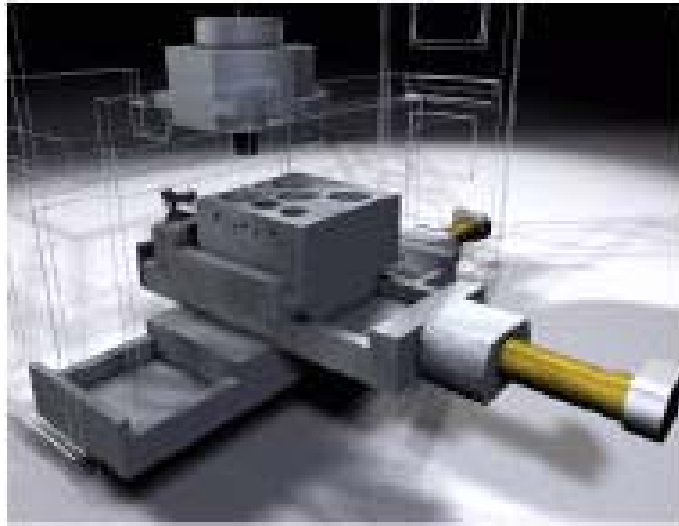


Figure 3. MTS Nano Instruments, Oak Ridge TN.

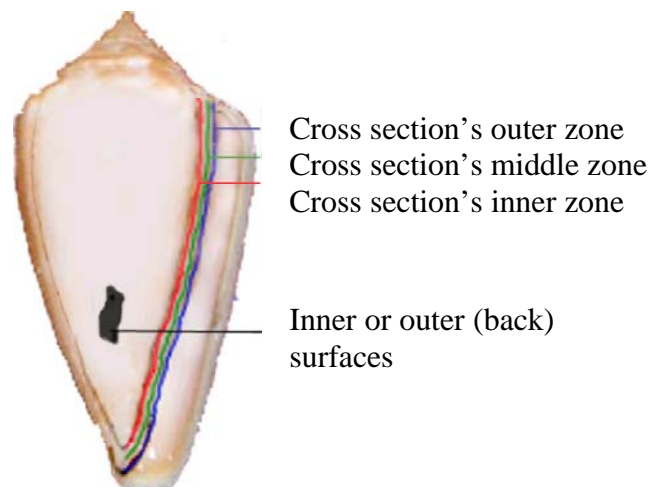


Figure 4. Indentation zones.

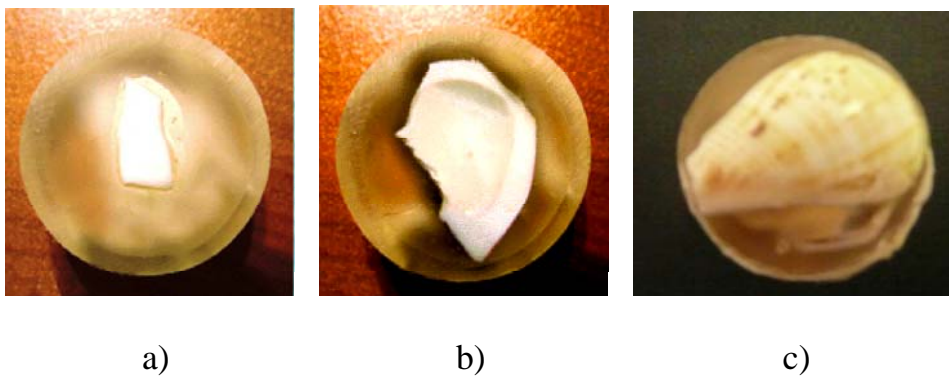


Figure 5. Specimens used: a) inner surface, b) cross section zones, c) outer surface.

were incorporated inside a resin support, Figure 5 and those of the cross section have been lapped in order to obtain a flat surface. On each of these surfaces the indentation has been performed at different maximum depths: from 250 nm to 4 μm , with a step of 250 nm. Both on the inner/outer surfaces and on each cross-sectional zone every test consisted of an indentation matrix 2x5: thus globally 800 indentations have been performed. In the choice of the area to indent the nanoindentation-boundary interaction has been avoided and, for each matrix, the distance between the indentation points has been increased proportionally to the indentation depth, in order to avoid their self-interactions.

The Oliver-Pharr method was used for data extraction [5]. According to this model, a loading-unloading cycle is applied and the measured maximum force, averaged on the corresponding indentation area, gives the hardness of the specimen while from the slope of the unloading curve, its Young's modulus can be derived. Each indentation was made using a diamond Berkovich tip, Figure 6.

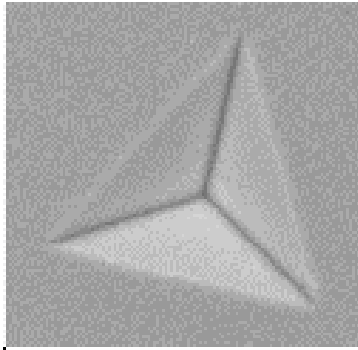


Figure 6. Berkovich tip used (elastic constants: Young modulus = 1140 GPa, Poisson's ratio = 0.07).

4. Results and discussion

Results obtained for nanohardness and Young's modulus are reported in Tables 1 and 2 or Figures 7. Each figure is related to one of the five tested surfaces and shows nanohardness and Young's modulus at 16 different depths. Each point on the diagram, described in Tables 1 and 2, represents the average value of the indentation matrix.

The numerous observations have been analysed applying an *ad hoc* modification of the Weibull Statistics [6], i.e. interpreting the cumulative probability function F , of finding zones with hardness (Young's modulus) smaller than $H(E)$ at an indentation depth h , according to:

$$F(< H) = 1 - e^{-\left(\frac{h}{h_0}\right)^n \left(\frac{H}{H_0}\right)^m} \quad (1)$$

Table 1. Young's modulus measurements: matrix mean values and standard deviations; IS (Inner surface), CI (Cross section inner zone), CM (Cross section middle zone), CO (Cross section outer zone), OS (Outer surface).

<i>Young's modulus [GPa]</i>					
<i>Depth [nm]</i>	<i>Indented Surface</i>				
	<i>IS</i>	<i>CI</i>	<i>CM</i>	<i>CO</i>	<i>OS</i>
250	81.279 ± 17.816	1.148 ± 0.370	71.655 ± 48.894	67.321 ± 32.026	83.946 ± 36.172
500	74.370 ± 18.576	0.811 ± 0.168	71.315 ± 27.448	64.372 ± 40.712	75.668 ± 28.860
750	72.426 ± 10.712	0.616 ± 0.136	74.650 ± 14.360	66.923 ± 27.956	80.058 ± 15.162
1000	68.667 ± 7.910	0.553 ± 0.208	78.856 ± 28.222	72.572 ± 18.380	79.559 ± 20.274
1250	70.714 ± 6.768	0.461 ± 0.070	73.304 ± 20.580	56.387 ± 27.206	74.599 ± 46.044
1500	52.981 ± 32.346	0.352 ± 0.084	61.911 ± 25.920	69.231 ± 15.104	76.422 ± 14.534
1750	49.288 ± 29.130	0.377 ± 0.054	71.338 ± 9.928	68.175 ± 28.194	76.038 ± 5.328
2000	63.450 ± 2.448	0.325 ± 0.086	71.174 ± 22.840	70.863 ± 10.676	77.272 ± 23.380
2250	52.015 ± 34.358	0.309 ± 0.050	71.822 ± 14.384	67.929 ± 6.502	73.014 ± 19.526
2500	59.701 ± 5.894	0.288 ± 0.092	65.045 ± 6.768	69.148 ± 8.270	75.154 ± 33.076
2750	56.869 ± 13.532	0.260 ± 0.076	69.830 ± 13.836	60.788 ± 6.416	70.583 ± 10.536
3000	55.101 ± 12.122	0.240 ± 0.060	67.038 ± 10.758	62.926 ± 9.312	70.721 ± 9.954
3250	60.612 ± 12.366	0.235 ± 0.066	66.316 ± 2.820	58.085 ± 8.288	73.558 ± 22.002
3500	54.667 ± 13.148	0.235 ± 0.052	63.516 ± 6.200	54.617 ± 9.722	65.840 ± 13.386
3750	55.266 ± 12.908	0.222 ± 0.058	62.770 ± 6.102	52.964 ± 7.564	64.727 ± 25.580
4000	60.041 ± 8.536	0.212 ± 0.042	62.323 ± 8.710	62.467 ± 4.316	65.531 ± 22.600

Table 2. Nanohardness measurements: matrix mean values and standard deviations; IS (Inner surface), CI (Cross section inner zone), CM (Cross section middle zone), CO (Cross section outer zone), OS (Outer surface).

<i>Hardness [GPa]</i>					
<i>Depth [nm]</i>	<i>Indented Surface</i>				
	<i>IS</i>	<i>CI</i>	<i>CM</i>	<i>CO</i>	<i>OS</i>
250	2.960 ± 1.938	0.225 ± 0.044	2.308 ± 2.458	1.891 ± 1.664	4.585 ± 3.238
500	2.355 ± 1.828	0.140 ± 0.096	2.045 ± 1.236	2.005 ± 1.944	4.198 ± 3.616
750	2.715 ± 1.110	0.105 ± 0.066	3.178 ± 1.376	2.461 ± 1.862	4.471 ± 2.134
1000	2.466 ± 0.612	0.118 ± 0.106	3.786 ± 2.900	2.922 ± 1.382	4.473 ± 2.740
1250	2.813 ± 0.762	0.097 ± 0.034	3.520 ± 1.878	1.863 ± 1.978	3.043 ± 3.058
1500	1.549 ± 1.678	0.061 ± 0.032	3.090 ± 2.320	2.947 ± 0.784	4.485 ± 1.770
1750	1.456 ± 2.204	0.096 ± 0.036	3.587 ± 0.996	2.924 ± 2.816	4.635 ± 0.742
2000	2.631 ± 0.406	0.080 ± 0.044	3.610 ± 2.276	3.344 ± 0.830	4.043 ± 3.270
2250	2.067 ± 2.530	0.074 ± 0.036	3.664 ± 1.538	4 ± 0.822	3.926 ± 2.394
2500	2.766 ± 0.760	0.085 ± 0.048	3.253 ± 0.554	4.257 ± 1.084	3.940 ± 3.792
2750	2.443 ± 1.028	0.082 ± 0.038	3.691 ± 1.594	3.422 ± 1.126	3.992 ± 1.368
3000	2.208 ± 1.360	0.068 ± 0.030	3.590 ± 0.860	2.837 ± 0.838	3.652 ± 1.678
3250	2.642 ± 1.278	0.071 ± 0.034	3.823 ± 0.482	3.846 ± 1.288	4.296 ± 2.304
3500	2.366 ± 1.838	0.073 ± 0.020	3.676 ± 0.718	3.332 ± 1.212	3.418 ± 1.926
3750	2.431 ± 1.280	0.071 ± 0.022	3.675 ± 0.664	3.395 ± 0.940	3.334 ± 2.788
4000	3.064 ± 1.292	0.060 ± 0.024	3.551 ± 0.986	2.893 ± 0.442	3.557 ± 2.474

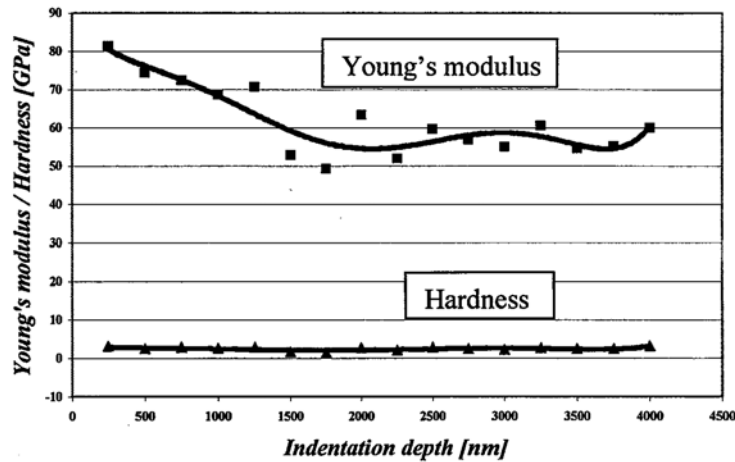


Figure 7a. Results obtained for nanohardness and Young's modulus, regarding tests performed on the inner surface of the shell.

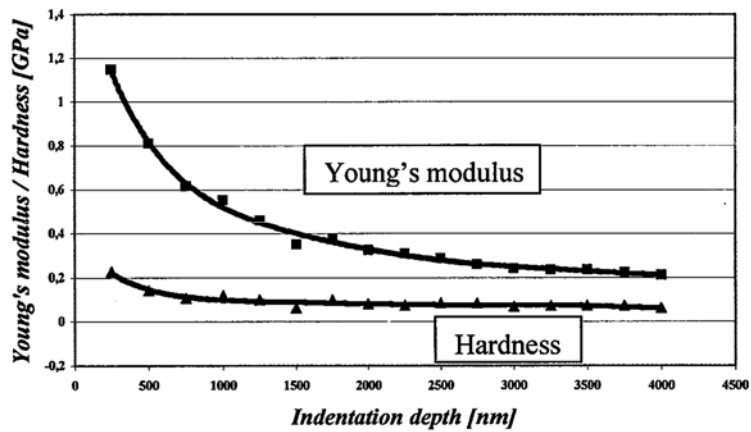


Figure 7b. Results obtained for nanohardness and Young's modulus, regarding tests performed on the inner zone of the cross section of the shell.

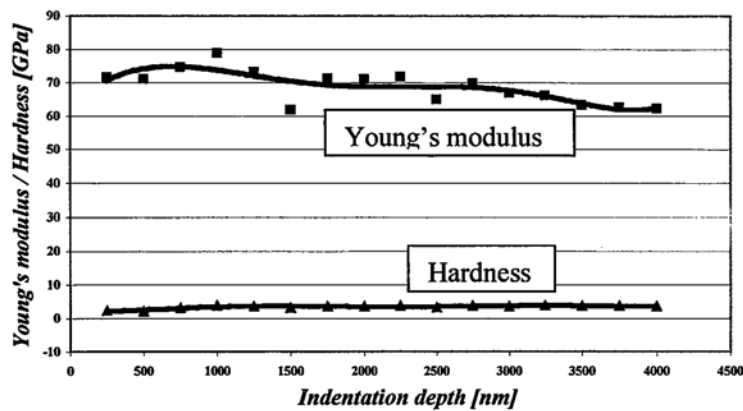


Figure 7c. Results obtained for nanohardness and Young's modulus, regarding tests performed on the middle zone of the cross section of the shell.

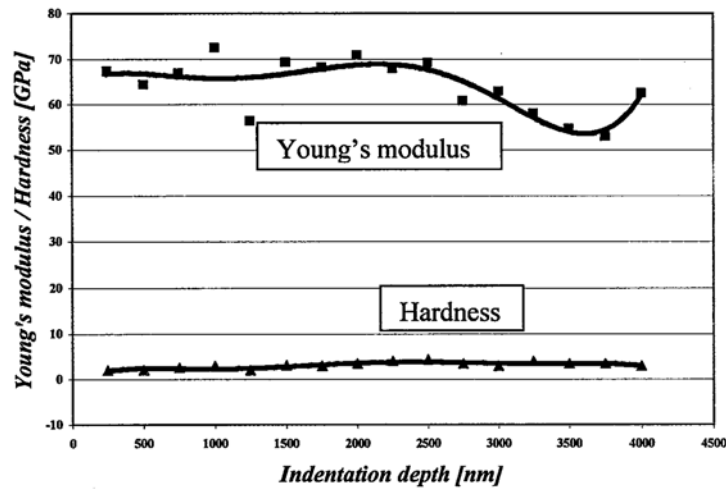


Figure 7d. Results obtained for nanohardness and Young's modulus, regarding tests performed on the outer zone of the cross section of the shell.

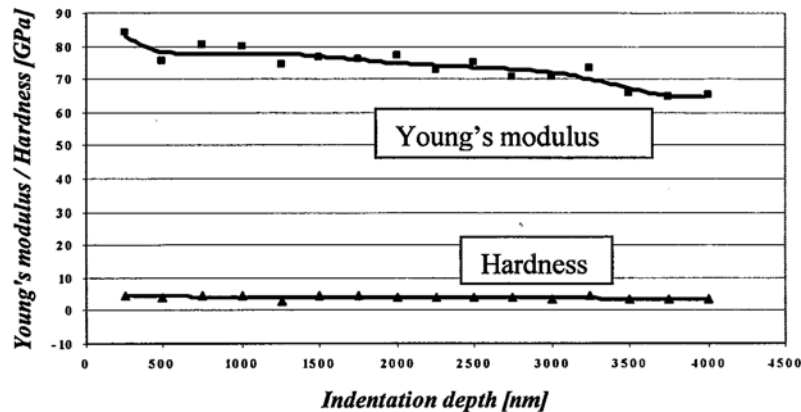


Figure 7e. Results obtained for nanohardness and Young's modulus, regarding tests performed on the outer surface of the shell.

where H_0 is the nominal hardness (or E_0 is the nominal Young's modulus, i.e. corresponding to $F = 63\%$, for $(h/h_0)^n = 1$), h_0 is a reference indentation depth (e.g. 1 micron), m is the Weibull modulus and n/m is the size-effect exponent. Classically Weibull Statistics is applied considering H as the material strength, h as a characteristic size defined as the cubic root of the fiber volume (or square root of the fiber surface), and thus $n=3$ (or $n=2$) for volume (or surface) predominant defects. Alternatively Nanoscale Weibull Statistics [7], specifically developed for nearly defect-free structures, consider $n=0$. Thus, we note that our modification proposed in eq. (1) describes, in addition to the hardness (Young's modulus) distribution, also the indentation size-effect, in the

form of $H \propto h^{-n/m}$ ($E \propto h^{-n/m}$). In our tests a negligible indentation size-effect has been revealed, thus suggesting $n=0$, for which in fact the highest statistical correlation (coefficient of correlation R^2) is found. An exception for the softer anisotropic inner layer is observed, for which we found the maximum statistical correlation for $n=3$, suggesting that the size-effect is governed by volume-dominated dislocation sliding. In fact $n=0$ would correspond for the nanohardness data analysis to $R^2(n=0) = 0.7232$, whereas $R^2(n=1) = 0.8755$, $R^2(n=2) = 0.9020$, $R^2(n=3) = 0.9028$, $R^2(n=4) = 0.8981$, thus with a maximum for $n=3$. The same finding can be observed for the Young's modulus, even if in such a case we have found R^2 increasing by monotonically increasing n (but $n>3$ has not a clear physical meaning). The results of our data analyses are reported in Table 3. As an example, the Weibull plots for the hardness measured along the two considered orthogonal directions of the inner anisotropic layer are shown in Figures 8. We conclude that the proposed modification of the Weibull Statistics is useful in treating nanoindentation experiments (see the coefficient of correlations of our fits in Table 3).

Moreover, the following considerations can be drawn: (i) a strong anisotropy of the inner layer is present: nanohardness and Young's modulus increase by one order of magnitude, from the cross-section to the surface; (ii) nanohardness and Young's modulus grow from the inner to the outer side, suggesting a natural evolution against external attacks, also improved by the softer and thus tougher anisotropic inner layer; (iii) no sensible difference has been observed as regards the nanoindentation depth, with the exception of the softer inner anisotropic layer, for which we have statistically deduced a volume-dominated dislocation sliding.

Table 3. Nanohardness (H) and Young's modulus (E) statistical data analysis. Coefficient of correlation R^2 , Weibull modulus m and nominal values H_0 , E_0 [GPa]. IS (Inner surface), CI (Cross section inner zone), CM (Cross section middle zone), CO (Cross section outer zone), OS (Outer surface); $h_0 = 1\mu\text{m}$; $n=0$ with the exception of $n=3$ at CI.

	<i>IS</i>	<i>CI</i>	<i>CM</i>	<i>CO</i>	<i>OS</i>
R_H^2	0.9380	0.9028	0.8312	0.9389	0.9737
m_H	5.7387	9.3303	6.3051	4.7326	9.6422
H_0	2.6328	0.1109	3.6423	3.3046	4.2112
R_E^2	0.8635	0.9639	0.8943	0.9639	0.9436
m_E	7.9092	6.8488	16.2630	12.5650	16.2130
E_0	65.5773	0.4975	71.1663	66.6810	76.3139

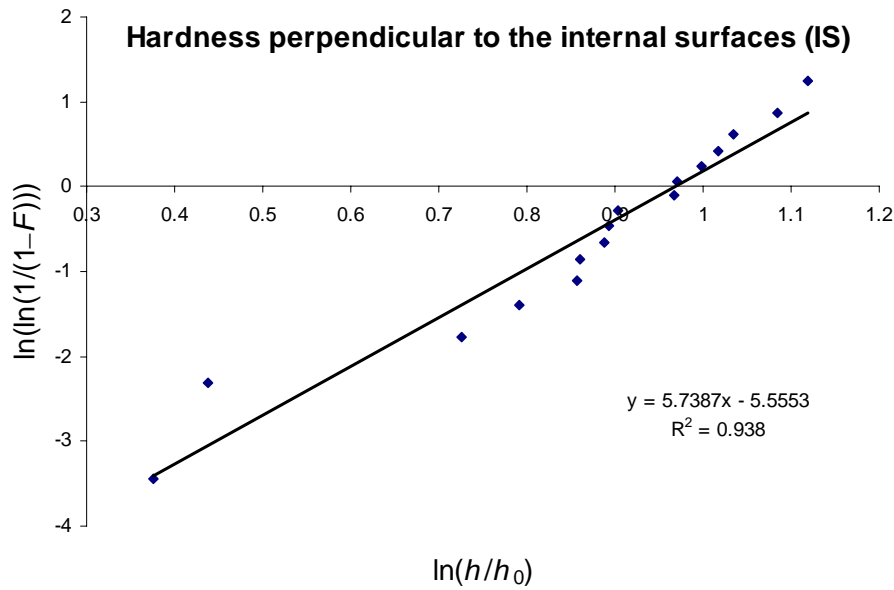


Figure 8a. Statistical data analysis on nanohardness measured on the inner surface of the shell ($n=0$).

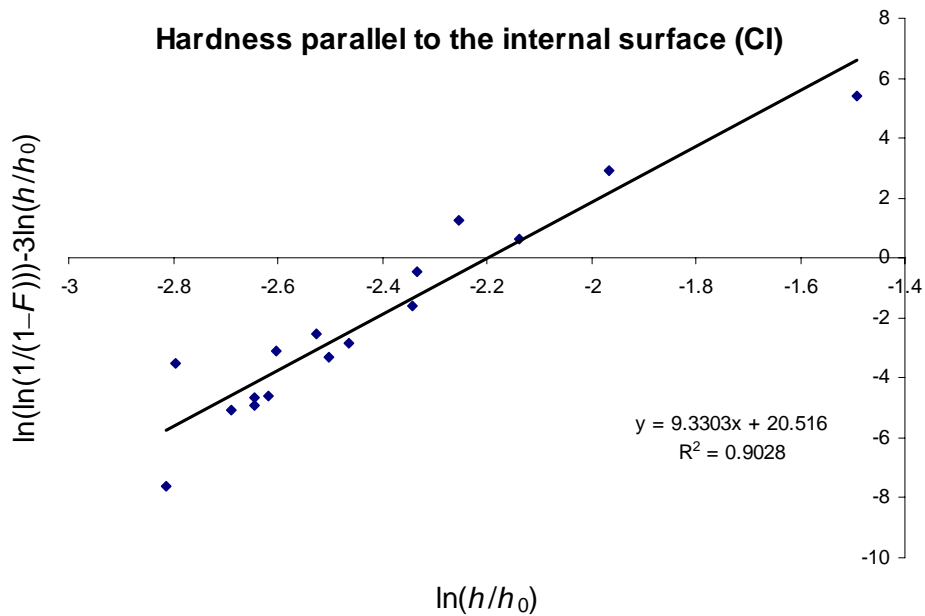


Figure 8b. Statistical data analysis on nanohardness measured on the cross section of the inner surface of the shell ($n=3$).

Concluding, our analysis supports the idea that super-composites or super-armors could be realised in the near future mimicking nacre [8], with anisotropic and hierarchical architectures composed by hard surface and tough volume.

5. References

1. Hou D.F., Zhou G.S. and Zheng M. 2004 *Conch shell structure and its effect on mechanical behaviors* BIOMATERIALS **25**(4) 751-756.
2. Kamat S., Kessler H., Ballarini R., Nassirou M. and Heuer A.H. 2004 *Fracture mechanism of the Strombous gigas conch shell: II-micromechanics analyses of multiple cracking and large-scale crack bridging* ACTA MATERIALIA **52** 2395-2406.
3. Lin A.Y.M., Meyers M.A. and Vecchio K.S. 2006 *Mechanical properties and structure of Strombous gigas, Tridacna gigas, and Haliotis rufescens sea shells: a comparative study* MATERIALS AND SCIENCE AND ENGINEERING C **26** 1380-1389.
4. Menig R., Meyers M.H., Meyers M.A. and Vecchio K.S. 2001 *Quasi-static and dynamical mechanical response of Strombous gigas (conch) shells*. MATERIALS AND SCIENCE AND ENGINEERING A **297** 203-211.
5. Oliver W.C. and Pharr G.M. 1992 *An improved technique for determining hardness and elastic modulus using load and displacement sensing indentation* J. MATER. RES. **7** 1564-83.
6. Weibull W. 1951 *A statistical distribution function of wide applicability* J. APPL. MECH. **18** 293-297.
7. Pugno N. 2006 *Mimicking nacre with super-nanotubes for producing optimized super-composites* NANOTECHNOLOGY **17** 5480-5484.
8. Pugno N. and Ruoff R. 2006 *Nanoscale Weibull statistics*. J. OF APPLIED PHYSICS **99** 024301/1-4.